PROCEEDINGS OF SCIENCE

Type Ia supernovae

Stan Woosley,[*†]
Department of Astronomy and Astrophsyics, UCSC, Santa Cruz, CA 95064
E-mail: woosley@ucolick.org

Dan Kasen, Haitao Ma, Gary Glatzmaier,
Department of Astronomy and Astrophsyics and Department of Earth and Planetary Sciences, UCSC, Santa Cruz, CA 95064
E-mail: kasen@ucolick.org,ma@ucolick.org,glatz@emerald.ucsc.edu

Andy Aspden, John Bell, Marc Day,
Center for Computational Sciences and Engineering, LBNL, Berkeley, CA 94720
E-mail: ajaspden@lbl.gov,jbbell@lbl.gov,msday@lbl.gov

Alan Kerstein, Vaidya Sankaran,
Combustion Research Facility, Sandia National Laboratories, Livermore, CA 94551
E-mail: arkerst@sandia.gov,vsankar@sandia.gov

and Fritz Röpke
Max Planck Institut für Astrophysik, Garching, Germany D-85741
E-mail: fritz@MPA-Garching.MPG.DE

Type Ia supernovae are the biggest thermonuclear explosions in the modern universe and responsible for making about 2/3 of the iron in our blood. They also play a special role as calibratable standard candles in cosmology, yet our understanding of them is primitive. We discuss reecent attempts in theory and simulation to describe more physically the ignition of the runaway in a carbon-oxygen white dwarf; the possible transition of burning to detonation; and the light curves, nucleosynthesis, and spectra of multi-dimensional models. The convection prior to ignition sets up a dipole-flow that implies off-center, lopsided ignition with an offset that depends on the rotation of the white dwarf. Once the flame ignites, an extended period of subsonic burning is followed by a transition to a detonation that happens when the burning enters the "stirred flame" regime. In terms of combustion parameters, the required conditions for detonation are Karlovitz numbers much greater than 10 and Damköhler numbers of approximately 10. Multi-dimensional models employing these ignition and detonation criteria give good agreement with the observed light curves and spectra of supernovae and with the observed width-luminosity relation. The data base generated by these models will be useful in planning future SN Ia survey missions.

10th Symposium on Nuclei in the Cosmos
July 27 - August 1 2008
Mackinac Island, Michigan, USA

[*]Speaker.

[†]This work has been supported by the DOE Scientific Discovery through Advanced Computing Program (DOE-DE-FC02-06ER41438). At Sandia, it was supported by the DOE Office of Basic Energy Sciences (DE-AC04-94-AL85000).

© Copyright owned by the author(s) under the terms of the Creative Commons Attribution-NonCommercial-ShareAlike Licence.

PoS(NIC X)047

1. Introduction

The "Type Ia supernova problem", how such supernovae explode and their observable properties, is actually a nested set of four problems, with the outcome of each depending on the results of the previous one. To a large extent, the problems are separable. First is the evolution leading to the runaway and the specific ignition kernel. In a carbon-oxygen white dwarf of nearly the Chandrasekhar mass, where does the temperature first exceed the threshold for explosive burning? Does ignition happen at many points or just one, and is ignition an ongoing process, or one that halts as soon as the first small region runs away? Second is the subsonic propagation of the flame. The hot ashes lie beneath cold fuel and the interface is unstable. Instabilities make turbulence that feeds back on the burning front telling it how to deform and move. How fast, on the large scale, does the burning move as a function of time, radius, and angle? Third, observations suggest that a subsonic flame (i.e., a deflagration) alone will not produce an adequate explosion. When and how does a transition to detonation occur? Does this transition happen many times in the explosion? Is the transition robust? Fourth and finally, having followed the hydrodynamics and nucleosynthesis, what does the supernova look like? What are its spectrum and light curve as a function of time?

Here we present new results for the ignition, detonation, nucleosynthesis, and radiation transport problems using a state-of-the-art approach to modeling the flame during the deflagration phase.

2. Ignition

We assume a "standard" model for a Type Ia supernova, a 1.38 $M_\odot$ carbon-oxygen white dwarf (typically 50% of each by mass) igniting at a central density of 2.9×10^9 g cm^{-3} and temperature $\sim 3 \times 10^8$ K. This so called "Chandrasekhar mass model" is thought to be an outcome of accretion from a binary companion whose properties are still poorly defined. Alternative sub-Chandrasekhar mass models [1] are not considered. Our calculations and those of others suggest that the spectra of such low mass explosions is unlike what is observed. Merging white dwarfs are an alternate scenario that might also lead to a progenitor not much larger than M_{ch} if magnetic torques are included [2, 3], though the full simulation has yet to be done.

Explosion does not occur upon first ignition, but is delayed by a few centuries as convection thaws out the cold white dwarf, raising the overall temperature [4] until a central value $\sim 7 \times 10^8$ K is reached [5]. At that point convection can no longer carry the increasing flux of energy released by the degenerate thermonuclear runaway and burning becomes localized, occurring in hot spots that develop temperature discontinuities at their boundaries. The flame is born.

Just where first ignition occurs dramatically affects the appearance of the subsequent supernova. Ignition closer to the center, gives a longer lasting, more energetic deflagration phase, and hence a weaker detonation phase, [6]. Ignition far off center gives the converse. An important recent result is the verification of a prediction by Chandrasekhar [7] that the convection prior to runaway is not isotropic, but has a dipole character. Three-dimensional studies by Kuhlen et al. [8] showed that this leads to lop sided ignition, off-center.

Those first 3D calculations were done in spectral coordinates with spherical symmetry, so the grid had a central singularity which required removing the innermost regions of the star from the simulation. We have now repeated Kuhlen's study using a 3D Cartesian grid (but still using

PoS(NIC X)047

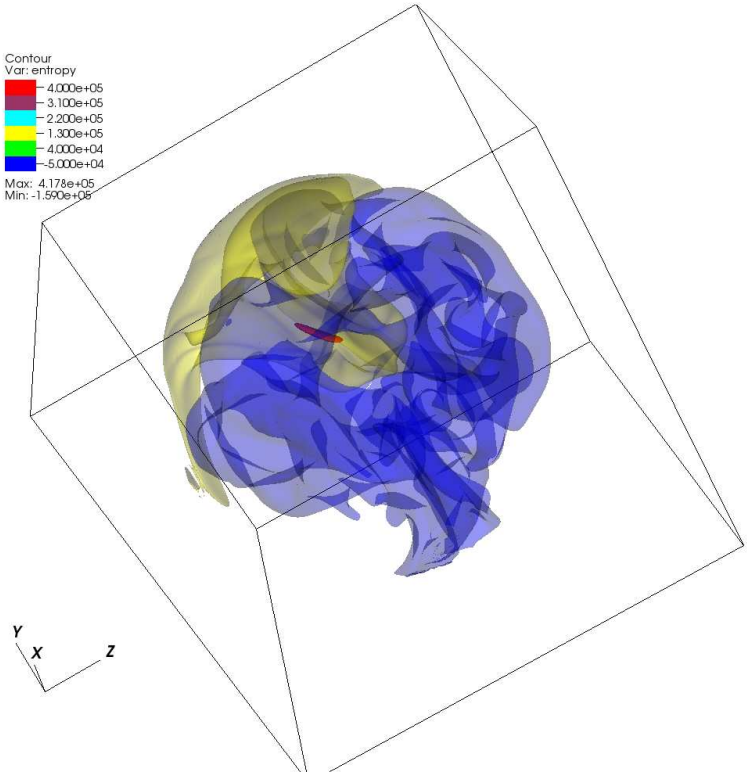

Figure 1: The distribution of entropy perturbations in a 3D anelastic simulation (384^3 zones) of the convection leading up to a Type Ia supernova explosion. The star is not rotating. Red color indicates regions of high entropy and maximal excess temperature (δT/T). The total temperature, T + δT, is greatest at the base of the red region, and that is where ignition occurs [9].

anelastic hydrodynamics) that has no coordinate singularity [9]. Our new results (Fig. 1) agree with his earlier findings. The maximum temperature is still found in an outflow on one side, displaced from the center by $\sim$100 km. Interestingly, calculations of the same star with the same code in 2D showed a very different ignition pattern. The dipole convective flow was still clearly present, but the hot spots developed in a torus around the jet where the flow stagnated. The 3D results, though low in resolution (Re $\sim$ 1000), are regarded as superior because of the well known tendency of 2D turbulence to cascade to artificially large scales. The calculation was also repeated with a mild amount of rotation, ω = 0.84 rad s^{-1}, or about 2% of break up. Even this relatively small amount of rotation affected the flow pattern. The dipole was still present, but fractured and twisted by the Coriolis force. Ignition still occurred a little off center on one side, but closer to the center. It may be that the brightness of a SN Ia is related to the rotation rate of the presupernova star. An important caveat is that the 3D calculations of Ma et al. have a rather low Reynolds number due to numerical viscosity, Re $\sim$1000. The actual Reynolds number in the star is about 10 orders of magnitude larger. Convection at such high values of Re may have a qualitatively different character and the dipole flow may be less pronounced [10, 11, 12]. We are currently repeating the calculation using a new 3D low-Mach number code, MAESTRO, developed for this purpose [13, 14].

PoS(NIC X)047

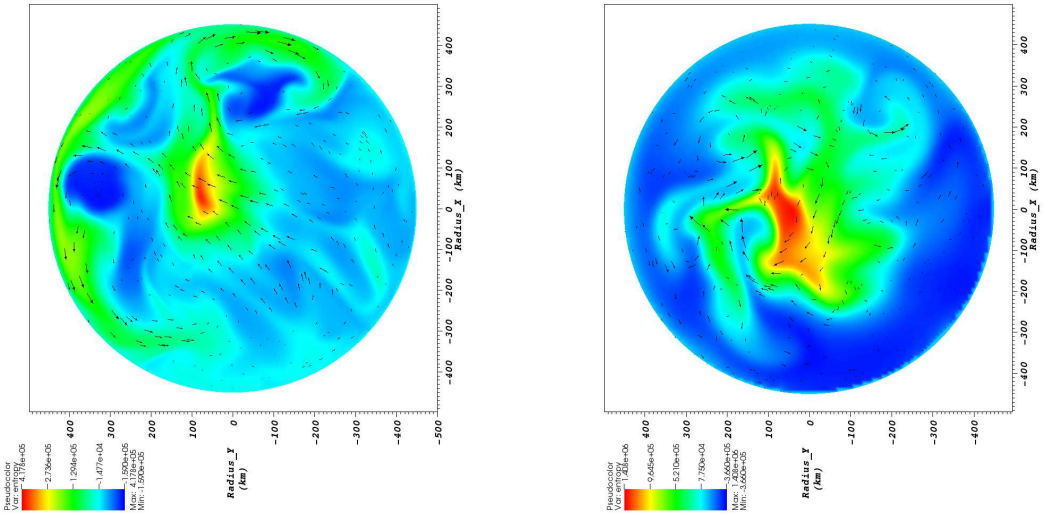

Figure 2: Flow patterns in 2D slices of the 3D calculation shown in Fig. 1 and an equivalent calculation that rotated with an angular speed of 2.52 rad s^{-1} (centrifugal force/gravity = 15%). The figures are color-coded by entropy-perturbation, yellow and red being highest. In the rotating model (right) the flow is more chaotic and the dipole flow not so apparent. The high temperature region almost overlaps the center [9].

3. Propagation

Once the flame is born, the computation enters a new phase where fluid instabilities and turbulence are the dominant effects and challenges. The hot ash is buoyant with respect to the cold fuel in which it is immersed. As it rises, shear gives rise to turbulence which cascades to smaller length scales where it affects the motion of the flame. For plumes with characteristic sizes of hundreds of kilometers this sets the integral length scale for turbulence to be about 10 km. Any physical description of the flame must either very finely resolve this length scale, or use a subgrid model for the turbulence - or both. Since the initial radius of the star is 1800 km, and growing rapidly as it explodes, sub-km resolution in 3D is not yet feasible (though it is a lot easier than trying to resolve the flame itself which is only 10^{-4} - 10^{-1} cm thick). We thus employ a subgrid model [15]. A survey of 2D models ignited at various distances from the center of the star is given in §5.

4. Detonation

It is widely believed that in order to explain the observations of especially the brightest Type Ia supernovae, nuclear burning that remains subsonic at all times (deflagration) is inadequate [16, 17]. There must be, at late times after the star has already expanded significantly, a transition to a more rapid form of burning, i.e., detonation. So far, “delayed detonation” has been introduced into the models as a free parameter, typically an *ad hoc* function of density and turbulent energy. We have recently explored the conditions that might lead to a low-density transition to detonation in analytic [18], and in 1D [19], and 3D [20, 21] simulations. The conclusion is that the prospects for delayed detonation are looking good. The necessary conditions are what is seen in the multi-dimensional models and the predicted density is close to that invoked in previous parametrized calculations.

PoS(NIC X)047

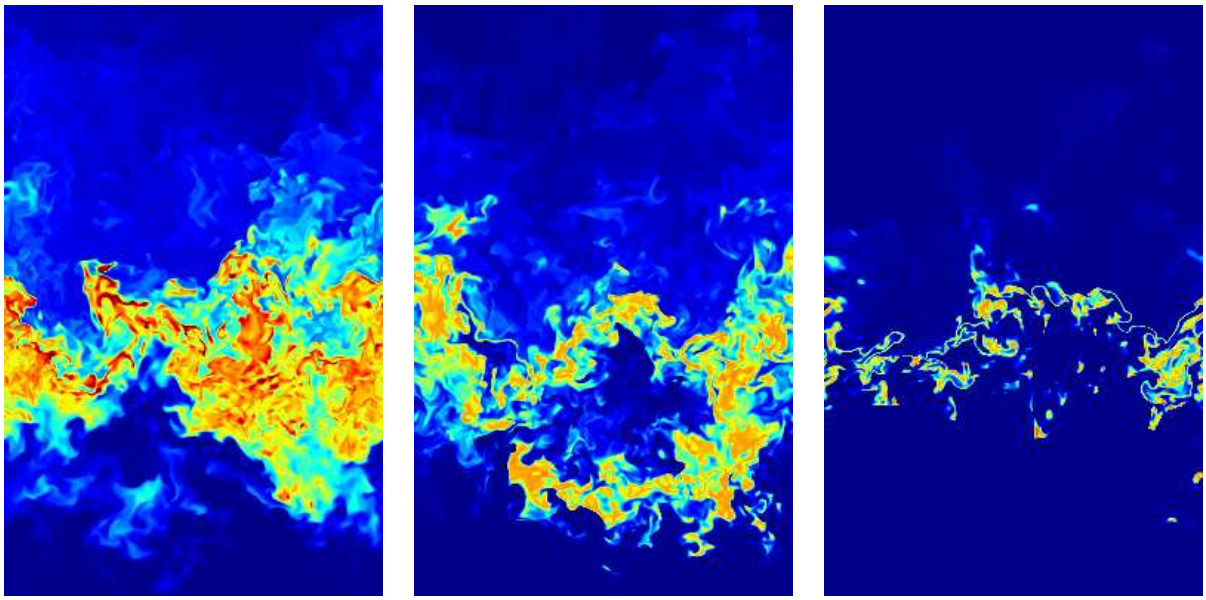

Figure 3: Instantaneous vertical slices of fuel consumption rate (intense burning in red, no burning in blue). As the flame burns in increasingly larger integral length scales, there is a decrease in the relative size of the flame structures, with burning occurring in distributed pockets. The whole domain width is shown but the height is cropped. The widths of the three calculations are 150 cm, 1200 cm, and 9600 cm.

4.1 3D Study

The work of Aspden et al. [20] focuses on flame in fuel that is 50% C, 50% O for a range of densities $1-8\times10^7$ g cm^{-3}. Flames are calculated in an assumed background of isotropic Kolmogorov turbulence with an energy dissipation rate, $U_L^3/L \sim 10^{15}$ erg g^{-1} s^{-1}, comparable to what is seen in the supernova for characteristic turbulent speeds of 100 km s^{-1} on a scale of 10 km. Their calculations use a 3D low Mach number code and clearly show a qualitative change in the nature of the burning at a density between 2 and 1 $\times10^7$ g cm^{-3}. At higher density the flame, though clearly distorted by the large scale eddies, still behaves like a laminar flame as anticipated by Damköhler [22]. However, as the density approaches 10^7 g cm^{-3}, the nature of the burning changes as small eddies penetrate the burning region and start to mix fuel and ash on a scale larger than the flame thickness. In terms used by the chemical combustion community, the Gibson length, the smallest eddy that can turn over on a burning time scale, becomes smaller than the flame thickness. That is, the Karlovitz number, Ka, which is the square root of the flame thickness to Gibson scale, becomes greater than 1.

More recent studies on larger length scales by Aspden et al as discussed in [21], show larger mixed structures being created as the calculation is extended to larger length scales of turbulence (Fig. 3). Unfortunately, even on current generation machines, a sufficiently large (10 km) 3D calculation with the necessary resolution is not feasible. We thus turn to 1D tools from the chemical combustion community for assistance.

4.2 1D Results Using LEM

The Linear Eddy Model (LEM) [23] is a numerical technique that captures many of the aspects

PoS(NIC X)047

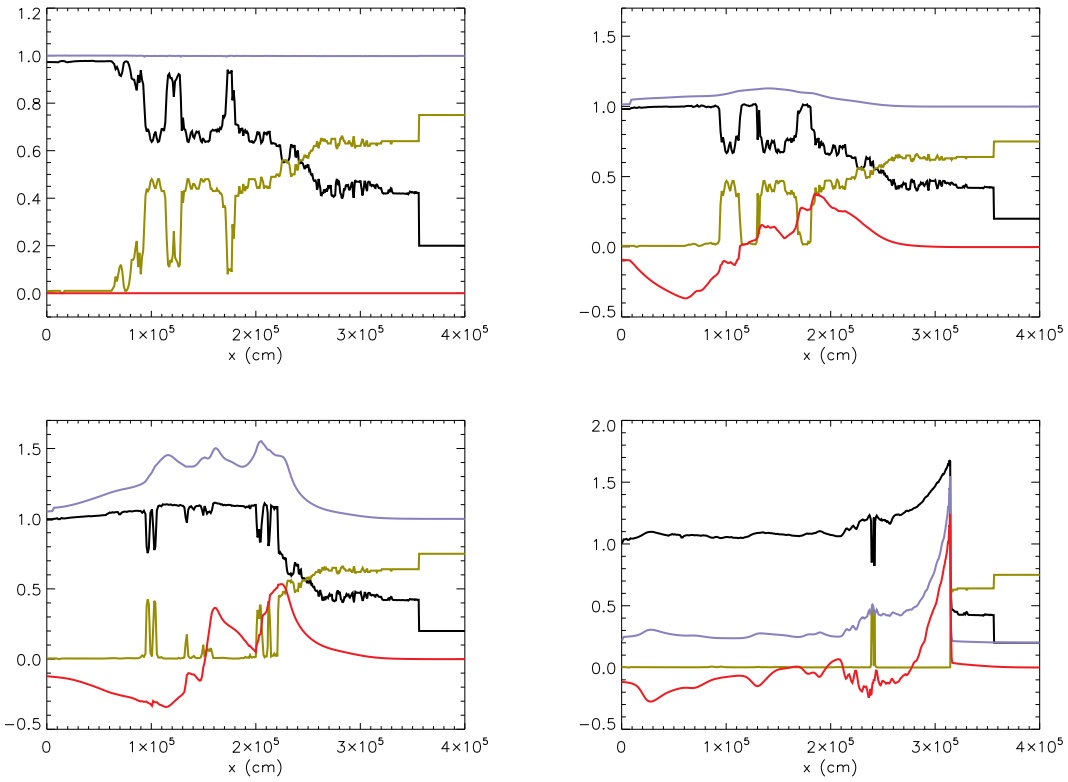

Figure 4: The birth of a detonation. A sample mixture calculated using LEM for a density 1.0×10^7 g cm^{-3}, u' = 500 km s^{-1}, and L = 10 km was mapped into a compressible hydrodynamics code and its subsequent evolution was followed. The time selected was characterized by a very subsonic flame speed but temperature gradients that looked "interesting". Following the remap, which preserved distance scale, ash was on the left and fuel on the right. A detonation developed that, barring large barriers of ash, would explode the whole star (see text). Shown in the plot are carbon mass fraction (gold), pressure (blue), temperature (black), and velocity (red) at four different times - 0, 0.15, 0.30, and 0.43 ms after the mapping. The velocity has been divided by 500 km s^{-1} in frames 1 and 2, 2000 km s^{-1} in frame 3 and 5000 km s^{-1} in frame 4. The pressure has been scaled by the background value, 9.08×10^{23} dyne, in frames 1, 2, and 3, and by an additional factor of 5 in frame 4. The temperature has been divided by 3.0×10^9 K.

of 3D turbulence on a 1D grid. A background isotropic turbulence obeying Kolmogorov statistics is assumed and the action of eddies on a field of abundances and temperature is represented by an instantaneous map (a so called "triplet map"). Eddy locations are random and size sampling is based on Kolmogorov scaling. The triplet map captures compressive strain and rotational folding effects of eddies and causes no property discontinuities. This approach simulates evolution along a 1D line-of-sight through a 3D flow.

The first frame of Fig. 4 shows the result of a calculation of a turbulent flame, also at 10^7 g cm^{-3}, modeled with LEM. The turbulent energy dissipation rate was somewhat larger than for the 3D study, 500 km s^{-1} on a length scale of 10 km, but still within the bounds expected in the supernova [24]. Conditions from an admittedly carefully selected point in the calculation were mapped into a compressible hydrodynamics code, Kepler [25], and the subsequent burning followed. Burn-

PoS(NIC X)047

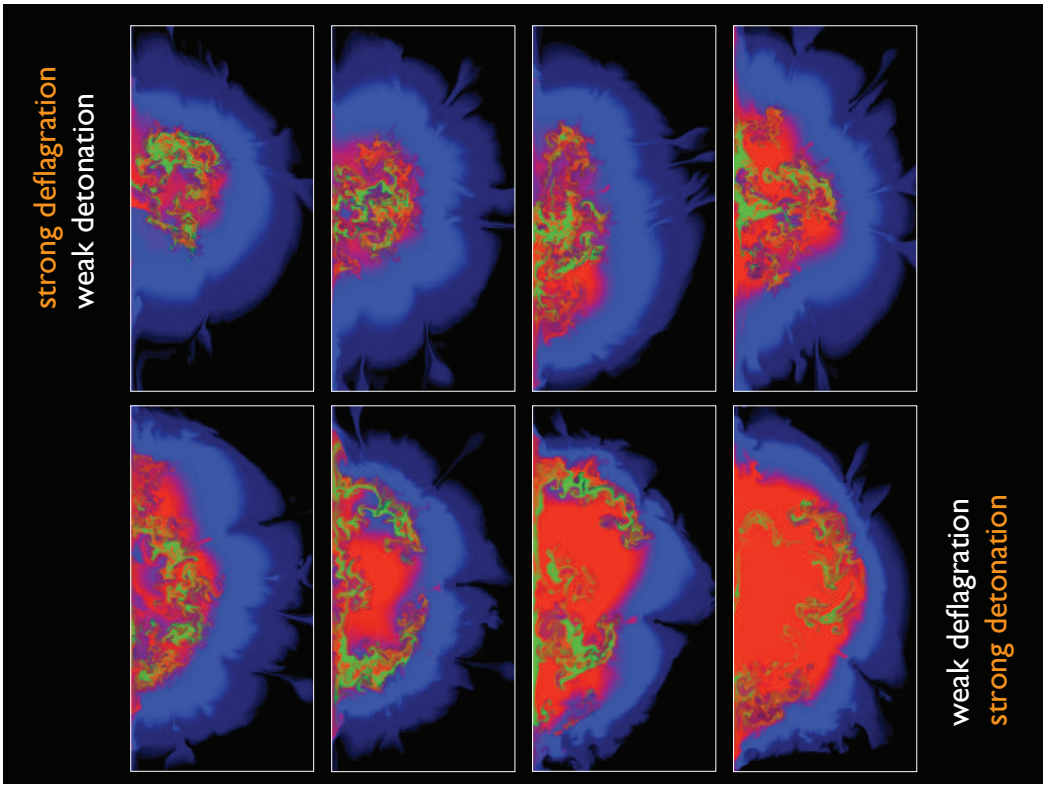

Figure 5: Chemical structure of the ejected debris for a subset of the explosion models which vary in ^{56}Ni mass. Blue represents intermediate mass elements (i.e., silicon, sulfur, calcium), green stable iron group elements, and red ^{56}Ni. The turbulent inner regions reflect fluid instabilities that develop during the deflagration phase of burning. Figure taken from Kasen et al [27].

ing of a small fraction of carbon at high temperature in the mixture occurred supersonically. This launched a pressure front, not yet a detonation, that was amplified by burning in the surrounding fuel-ash mixture. Because of the generally monotonic decline of the burning temperature over a distance of almost a km, the strength of the burning and overpressure grew until a strong detonation wave was present. This wave then propagated successfully off of the grid and, presumably, through the remainder of the star.

A variety of conditions must occur simultaneously for detonation to happen. None are overly restrictive, but the combination is a rare occurrence. That is OK since there are many opportunities realized on a 10 km scale across the flame front, which may be 1000's of km in size by the time the detonation happens. The first condition is that the fastest turbulent fluctuations must already move at a substantial fraction of the sound speed. 500 km s^{-1} seems a minimum; the sound speed at the relevant density is about 4000 km s^{-1}. The flame must be torn by the turbulence, hence Karlovitz numbers greater than 10 are required, but more than that, the mixed structures must be large enough to initiate and sustain a detonation. This requires the density to be low enough that large eddies can turnover without burning. A measure of the burning in a large eddy turnover time

PoS(NIC X)047

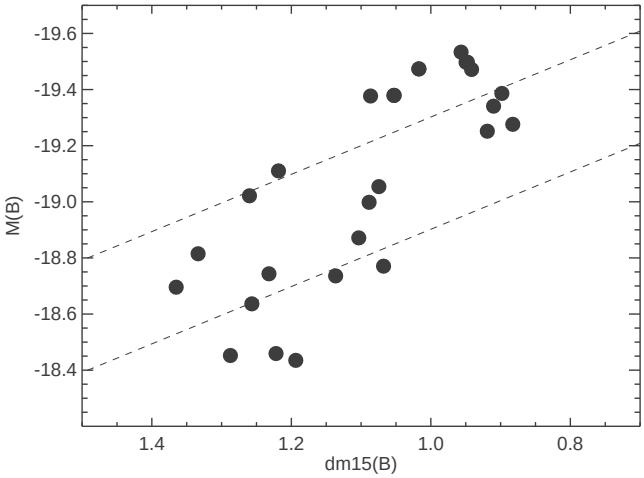

Figure 6: Relation between the peak B-band brightness (measured in the logarithmic magnitude scale) and light curve decline rate, here quantified using the decline in brightness measured from peak to 15 days after peak. The dashed band indicates, approximately, the observed width luminosity relation and its spread. Figure from Kasen et al. [27].

is the Damköhler number, Da. It seems that Da $\sim$ 10 is necessary [19].

5. Survey

Based upon the general results of §2 and §4, thirty 2D models of Type Ia supernovae were calculated [26]. Burning was ignited in a variable solid angle, displaced slightly from the center. Specifically, 20 to 150 ignition points were chosen randomly distributed from the center out to $\sim$300 km and in a solid angle whose opening varied from 60 degrees to 360 degrees. Most of the calculations had a large solid angle.

5.1 Light Curves and Spectra

The post-explosion evolution of each supernova was calculated [27] using a time-dependent multi-dimensional radiation transport code [28]. For each model, the synthetic broadband light curves and spectral time series were determined as observed from 30 different viewing angles and the results were averaged. The theoretical predictions are in good agreement with the observed properties of typical events, offering additional strong support for some sort of delayed detonation model of SNe Ia explosions. The peak bolometric luminosities vary from 0.6 to 2.0 x 10^{43} erg s^{-1}, spanning the range of luminosities observed in SNe Ia, excepting the most extreme sub-luminous and super-luminous events. Without any artificial tuning, the luminosity of the models correlates with light curve shape, giving a width-luminosity-relation (WLR) similar to what is observed. In Fig. 6 the B-band peak magnitudes (MB) are plotted versus the post-maximum light curve decline rate (ΔM_{15}).

PoS(NIC X)047

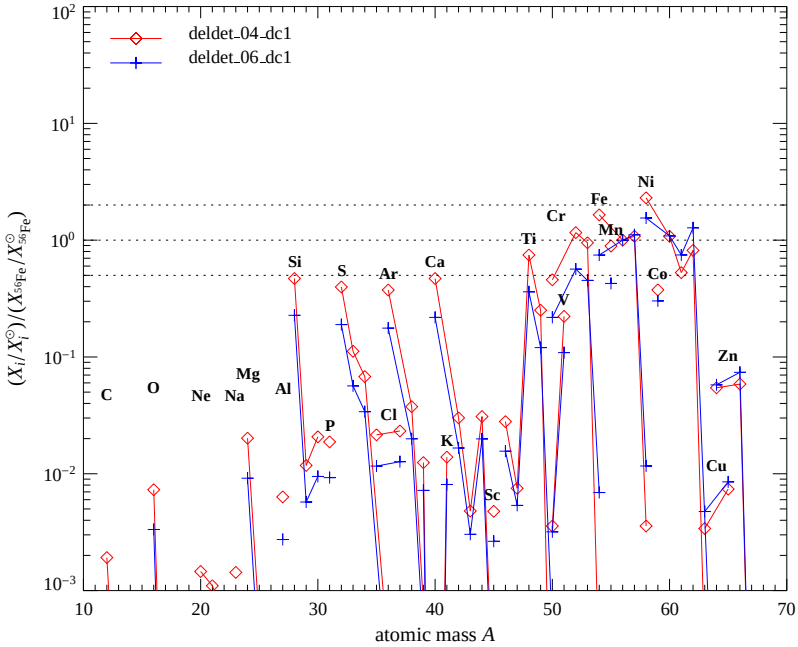

Figure 7: Nucleosynthesis in two models [26]. The blue points are for an explosion that made 0.94 $M_{\odot}$ of ^{56}Ni. The red points are for one that made 0.70 $M_{\odot}$ of ^{56}Ni. Figure from Röpke et al [26].

5.2 Nucleosynthesis

The nucleosynthesis from two representative models is given in Fig. 7. These calculations used an initial metallicity of 0.5 solar, though the results are not very sensitive to that assumption. Both models show reasonable agreement with the solar elemental abundance pattern in the iron group, but only the brighter models reproduce the isotopes of iron and nickel well. For the lower energy explosion, more nucleosynthesis occurs in the deflagration phase and electron capture at high density overproduces ^{54}Fe and ^{58}Ni. For the higher energy explosion, a greater fraction of ^{56}Fe is made (as ^{56}Ni) by detonation at low density. Brighter models also produce less manganese and titanium and there might be diagnostics of this in the history of these two elements in metal deficient stars in our Galaxy. These good agreement of ^{54}Fe/^{56}Fe and ^{58}Ni/^{56}Fe for only the model that makes more ^{56}Ni suggests that the typical SN Ia in the history of the Milky Way Galaxy has been a bright one, with low luminosity events comparatively rare. This is consistent with observations that suggest that SN Ia in spiral and star forming galaxies are often brighter than in ellipticals [29].

PoS(NIC X)047

References

[1] Woosley, S. E., & Weaver, T. A. 1994, *Ap. J.*, 423, 371

[2] Yoon, S.-C., Podsiadlowski, P., & Rosswog, S. 2007, *Mon. Not. Roy. Astron. Soc.*, 380, 933

[3] Suijs, M. P. L., Langer, N., Poelarends, A.-J., Yoon, S.-C., Heger, A., & Herwig, F. 2008, *Astron, & Ap.*, 481, L87

[4] Baraffe, I., Heger, A., & Woosley, S. E. 2004, *Ap. J.*, 615, 378

[5] Woosley, S. E., Wunsch, S., & Kuhlen, M. 2004, *Ap. J.*, 607, 921

[6] Röpke, F. K., Woosley, S. E., & Hillebrandt, W. 2007, *Ap. J.*, 660, 1344

[7] Chandrasekhar, S. 1961, Hydrodynamic and Hydromagnetic Stability, Dover Publ., New York, P.220ff

[8] Kuhlen, M., Woosley, S. E. & Glatzmaier, G. A. 2006, *Ap. J.*, 640, 407

[9] Ma, H., Woosley, S. E., Glatzmaier, G., & Evonuk, M. 2008, *Ap. J.*, in preparation.

[10] Kraichnan, R. H. 1962, Phys. of Fluids, 5, 1374

[11] Kadanoff, L. P. 2001, Physics Today, 54(8), 34

[12] Lantz, S. R., & Fan, Y. 1999, *Ap. J.*, 121, 247.

[13] Almgren, A. S., Bell, J. B., Rendleman, C. A., & Zingale, M. 2006, *Ap. J.*, 637, 922 and 649, 927

[14] Almgren, A. S., Bell, J. B., Nonaka, A., & Zingale, M. 2008, *Ap. J.*, 684, 449

[15] Niemeyer, J., & Hillebrandt,W 1995, *Ap. J.*, 452, 769

[16] Höflich, P., & Khokhlov, A. 1996, *Ap. J.*, 457, 500

[17] Kozma, C., Fransson, C., Hillebrandt, W., Travaglio, C., Sollerman, J., Reinecke, M., Röpke, F. K., & Spyromilio, J. 2005, *Astron, & Ap.*, 437, 983

[18] Woosley, S. E. 2007, *Ap. J.*, 668, 1109

[19] Woosley, S. E., Kerstein, A., Sankaran, V., and Röpke, F. 2008, *Ap. J.*in preparation

[20] Aspden, A., Bell, J. B., Day, M. S., Woosley, S. E., and Zingale, M. 2008, *Ap. J.*, in press

[21] Woosley, S. E., et al. 2008, Journal of Physics Conference Series, in press

[22] Damköhler G. 1940 *Z. Elektrochem* 46, 601 – 652

[23] Kerstein, A. 1991, J. Fluid Mech., 231, 361

[24] Röpke, F. K. 2007, *Ap. J.*, 668, 1103

[25] Weaver, T. A., Woosley, S. E., & Zimmerman, G. B. 1978, *Ap. J.*, 225, 1021

[26] Röpke, F. et al., 2008, *Ap. J.*, in preparation.

[27] Kasen, D., Röpke, F., & Woosley, S. E. 2008, in preparation.

[28] Kasen, D., Thomas, R. C., & Nugent, P. 2006, *Ap. J.*, 651, 366

[29] Gallagher, J. S., Garnavich, P. M., Berlind, P., Challis, P., Jha, S., & Kirshner, R. P. 2005, *Ap. J.*, 634, 210

PoS(NIC X)047